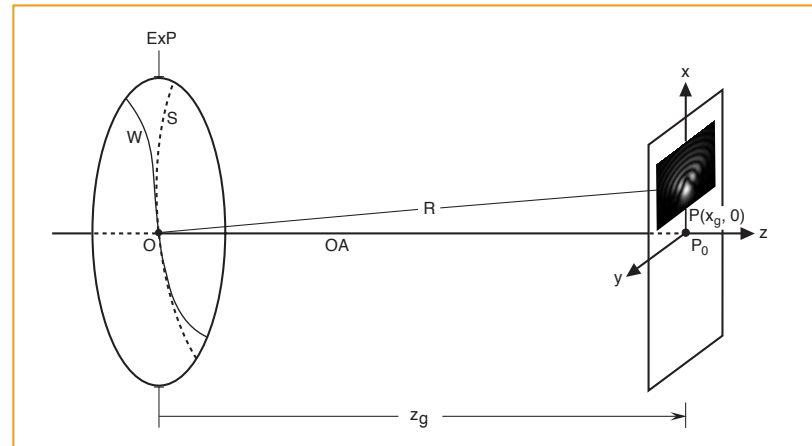


# Optical Imaging and Aberrations



© Virendra N. Mahajan

Adjunct Professor  
College of Optical Sciences  
University of Arizona

The Aerospace Corporation  
El Segundo, California 90245  
(310) 336-1783

[virendra.n.mahajan@aero.org](mailto:virendra.n.mahajan@aero.org)

**Lecture 18. Incoherent Vs Coherent Imaging**

# Lecture 18 Summary

## Incoherent Vs Coherent Imaging

- Coherent Imaging
  - By a System With a Circular Pupil
- Two-Point Resolution
- Line-Spread Function (LSF)
- Edge-Spread Function (ESF)
- Image of a Disc
- Image of a General Extended Object
- Use of a Lens for Obtaining Fourier Transforms

## Incoherent Vs Coherent Imaging

For an incoherently illuminated object, the complex amplitudes from its elements bear randomly varying time relationships. Hence, the image is linear in irradiance, and the irradiance distribution of the image is obtained by superimposing the irradiance distributions of the image elements.

For a coherently illuminated object, the complex amplitudes from its elements bear a time-independent relationship among them. Hence, the image is linear in complex amplitude, and the complex amplitude distribution of the image is obtained by superimposing the complex amplitude distributions of the image elements.

There is no distinction between the (irradiance) images of an incoherently or coherently illuminated point object. Hence, we look for the differences between the images of incoherently and coherently illuminated two points, a line, an edge, a disc, and a general extended object.

But, first we discuss the fundamentals of coherent imaging.

## Coherent Imaging

### Coherent spread function (CSF)

Let  $G(\vec{r}_p; \vec{r}_o)$  be the relative pupil function of an imaging system representing the complex amplitude in the plane of its exit pupil due to a unit amplitude of an object element centered at  $\vec{r}_o$  per unit area of the object element at a distance  $z_o$  from the entrance pupil.

Amplitude object:  $U_o(\vec{r}_o)$

Amplitude image:

Complex amplitude distribution in an observation plane at a distance  $z_i$  from the plane of the exit pupil [from Eq. (1-49)]:

$$\begin{aligned} U_i(\vec{r}_i; z_i) &= \int \Delta U_i(\vec{r}_i; \vec{r}_o; z_i) \\ &= -\frac{i}{\lambda z_i} \exp\left[ik\left(z_i - z_g + \frac{r_i^2}{2z_i}\right)\right] \int d\vec{r}_o U_o(\vec{r}_o) \exp\left(-ik\frac{r_o^2}{2z_o}\right) \\ &\quad \times \int G(\vec{r}_p; \vec{r}_o; z_i) \exp\left[-\frac{2\pi i}{\lambda z_i} \vec{r}_p \cdot \left(\vec{r}_i - \frac{z_i}{z_g} \vec{r}_g\right)\right] d\vec{r}_p \quad (1-236) \end{aligned}$$

where  $\vec{r}_g = M\vec{r}_o$  is the position vector of the Gaussian image point with a magnification  $M$ ,  $z_g$  is the distance of the Gaussian image plane, and the defocused pupil function is

$$G(\vec{r}_p; \vec{r}_o; z_i) = G(\vec{r}_p; \vec{r}_o) \exp\left[\frac{ik}{2} \left(\frac{1}{z_i} - \frac{1}{z_g}\right) r_p^2\right]$$

Point object located at  $\vec{r}_j$  with an amplitude  $U_j$ :

$$U_o(\vec{r}_o) = U_j \delta(\vec{r}_o - \vec{r}_j)$$

$$\therefore U_i(\vec{r}_i; \vec{r}_j; z_i) = U_j CSF(\vec{r}_i; \vec{r}_j; z_i)$$

where

$$CSF(\vec{r}_i; \vec{r}_j; z_i) = -\frac{i}{\lambda z_i} \exp\left\{ik \left[ (z_i - z_g) + \frac{1}{2} \left( \frac{r_i^2}{z_i} + \frac{r_j^2}{z_o} \right) \right]\right\} \\ \times \int G(\vec{r}_p; \vec{r}_o; z_i) \exp\left[-\frac{2\pi i}{\lambda z_i} \vec{r}_p \cdot \left( \vec{r}_i - \frac{z_i}{z_g} M\vec{r}_j \right)\right] d\vec{r}_p$$

is the **coherent (point-) spread function** of the system.

Now, we make certain approximations so that the amplitude distribution in an observation plane is equal to the convolution of the corresponding distribution of the Gaussian image and the CSF.

As in the case of incoherent imaging, we assume that the object is small enough that the relative pupil function  $G(\vec{r}_p; \vec{r}_o; z_i)$  does not vary significantly with the location  $\vec{r}_o$  of an object element; i.e., we assume that the system is **isoplanatic** for the small object under consideration.

Thus, we replace  $G(\vec{r}_p; \vec{r}_o; z_i)$  by  $G(\vec{r}_p; z_i)$  for a small isoplanatic object.

In practice, the **Fresnel number** of imaging systems is quite large, resulting in a very small depth of focus. Hence, we may replace  $z_i$  by  $z_g$ , except in determining the defocus aberration, which varies as  $r_p^2$ .

For systems with small **fields of view**, we may replace  $z_g$  by  $R$ , the radius of curvature of the Gaussian reference sphere with respect to which the aberration is defined.

**For coherent imaging, we must consider another approximation, namely, that the variation of the quadratic phase factor  $\exp\left[-ik\left(r_o^2/2z_o\right)\right]$  depending on  $\vec{r}_o$  is negligible.**

Since the magnitude of the CSF is significant only in a small region (on the order of the Airy disc) surrounding the Gaussian image point, therefore, at a particular point of observation  $(\vec{r}_i; z_i)$ , the contributions of the quadratic phase factor will come from a small region of the object.

Hence, we may replace  $\vec{r}_o = \vec{r}_g/M$  by  $\vec{r}_i/M$  in the object-dependent quadratic phase factor  $\exp\left[-ik\left(r_o^2/2z_o\right)\right]$ . Moreover, any phase factors that do not depend on the location of the object point can be dropped when the measured quantity in the observation plane is the irradiance.

In view of the above approximations:

$$CSF(\vec{r}_i; \vec{r}_j; z_i) = -\frac{i}{\lambda R} \int G(\vec{r}_p; z_i) \exp\left[-\frac{2\pi i}{\lambda R} \vec{r}_p \cdot (\vec{r}_i - M\vec{r}_j)\right] d\vec{r}_p$$

- Integral on the right-hand side depends on the position vectors  $\vec{r}_i$  and  $\vec{r}_g$  of the observation and Gaussian image points, respectively, through their difference  $\vec{r}_i - \vec{r}_g$  only.
- Hence, we may replace  $CSF(\vec{r}_i; \vec{r}_j; z_i)$  by  $CSF(\vec{r}_i - M\vec{r}_j; z_i)$ .

- Thus, CSF is shift invariant in that its form does not depend on the location of the object point. A shift in the location of a point object merely shifts the whole image distribution by virtue of being centered at  $\vec{r}_g = M\vec{r}_j$ .

Isoplanatic coherent object of amplitude  $U_o(\vec{r}_o)$ :

Gaussian amplitude image (ignoring constant factors, e.g., area of entrance pupil):

$$U_g(\vec{r}_g) = M^{-1} U_o(\vec{r}_g/M)$$

Diffraction amplitude image: Equation (1-236) reduces to

$$\begin{aligned} U_i(\vec{r}_i; z_i) &= M^{-1} \int U_o(\vec{r}_g/M) CSF(\vec{r}_i - \vec{r}_g; z_i) d\vec{r}_g \\ &= \int U_g(\vec{r}_g) CSF(\vec{r}_i - \vec{r}_g; z_i) d\vec{r}_g \quad (1-242) \end{aligned}$$

where

$$CSF(\vec{r}_i; z_i) = -\frac{i}{\lambda R} \int G(\vec{r}_p; z_i) \exp\left(-\frac{2\pi i}{\lambda R} \vec{r}_p \cdot \vec{r}_i\right) d\vec{r}_p$$

- **CSF is proportional to an inverse Fourier transform of the pupil function (Theorem 22), and the amplitude image is convolution of the Gaussian amplitude image and the CSF (Theorem 23a).**

## Coherent transfer function (CTF)

Fourier transforming both sides of Eq. (1-242):

$$\begin{aligned}\tilde{U}_i(\vec{v}_i) &= \int d\vec{r}_i \exp(2\pi i \vec{v}_i \cdot \vec{r}_i) \int U_g(\vec{r}_g) CSF(\vec{r}_i - \vec{r}_g) d\vec{r}_g \\ &= \int d\vec{r}_g U_g(\vec{r}_g) \exp(2\pi i \vec{v}_i \cdot \vec{r}_g) \int CSF(\vec{r}_i - \vec{r}_g) \exp[2\pi \vec{v}_i \cdot (\vec{r}_i - \vec{r}_g)] d\vec{r}_i \\ &= \tilde{U}_g(\vec{v}_i) CTF(\vec{v}_i)\end{aligned}$$

where the **coherent transfer function** is

$$CTF(\vec{v}_i) = \int CSF(\vec{r}_i) \exp(2\pi \vec{v}_i \cdot \vec{r}_i) d\vec{r}_i$$

and the spectra of the amplitude diffraction and Gaussian images are

$$\tilde{U}_i(\vec{v}_i) = \int U_i(\vec{r}_i) \exp(2\pi \vec{v}_i \cdot \vec{r}_i) d\vec{r}$$

$$\tilde{U}_g(\vec{v}_i) = \int U_g(\vec{r}_i) \exp(2\pi \vec{v}_i \cdot \vec{r}_i) d\vec{r}$$

- **Spectrum of the diffraction amplitude image is given by the product of the spectrum of the Gaussian amplitude image and the CTF (Theorem 23b).**

Substituting for  $CSF(\vec{r}_i)$  and dropping the constant phase factor  $-i$ :

$$\begin{aligned}
 CTF(\vec{v}_i) &= \frac{1}{\lambda R} \int d\vec{r}_i \exp(2\pi\vec{v}_i \cdot \vec{r}_i) \int G(\vec{r}_p) \exp\left(-\frac{2\pi i}{\lambda R} \vec{r}_p \cdot \vec{r}_i\right) d\vec{r}_p \\
 &= \frac{1}{\lambda R} \int d\vec{r}_p G(\vec{r}_p) \int d\vec{r}_i \exp\left[2\pi i \vec{r}_i \cdot \left(\vec{v}_i - \frac{\vec{r}_p}{\lambda R}\right)\right] \\
 &= \frac{1}{\lambda R} \int d\vec{r}_p G(\vec{r}_p) \delta\left(\vec{v}_i - \frac{\vec{r}_p}{\lambda R}\right) \\
 &= G(\lambda R \vec{v}_i)
 \end{aligned}$$

- Thus, the **coherent transfer function is simply a scaled version of the relative pupil function (Theorem 24)**.
- If the system is diffraction limited, i.e., if it is aberration free, and its transmission across the exit pupil is uniform so that  $G(\vec{r}_p)$  is constant across the pupil (whose value varies inversely with the distance  $z_o$  of the entrance pupil from the object), then the normalized CTF is unity for those frequencies for which  $\lambda R \vec{v}_i$  lies inside the exit pupil.

## Relationship between incoherent and coherent spread and transfer functions

$$PSF(\vec{r}_i) = \frac{|CSF(\vec{r}_i)|^2}{\int |G(\vec{r}_p; z_i)|^2 d\vec{r}_p}$$

- PSF is the normalized modulus square of the CSF.

Fourier transforming:

$$\tau(\vec{v}_i) = \int G(\vec{r}_p) G^*(\vec{r}_p - \lambda R \vec{v}_i) d\vec{r}_p / \int |G(\vec{r}_p)|^2 d\vec{r}_p$$

Thus, the **incoherent transfer function OTF** is the (normalized) **autocorrelation of the coherent transfer function CTF**.

Since the pupil functions  $P$  and  $G$  are proportional to each other,  $G$  can be replaced by  $P$  to obtain the **OTF as the autocorrelation of the pupil function**.

## Coherent Imaging by a System With a Circular Pupil

### Coherent spread function

Coherent spread function representing the amplitude image of a point object observed in the Gaussian image plane:

$$CSF(\vec{r}_i) = \frac{1}{\lambda R} \int G(\vec{r}_p) \exp\left(-\frac{2\pi i}{\lambda R} \vec{r}_p \cdot \vec{r}_i\right) d\vec{r}_p$$

where we have omitted the factor  $-i$  in front of the right-hand side of the equation.

For an aberration-free system with a circular exit pupil of radius  $a$ , the relative pupil function is constant, say  $G_o$ , that is inversely proportional to  $z_o$ :

$$\begin{aligned} G(\vec{r}_p) &= G_o \quad , \quad \text{for } |\vec{r}_p| \leq a \\ &= 0 \quad , \quad \text{otherwise} \end{aligned}$$

$$\begin{aligned}
\therefore CSF(\vec{r}_i) &= \frac{G_o}{\lambda R} \int_0^a r_p dr_p \int_0^{2\pi} \exp\left[-\frac{2\pi i}{\lambda R} r_p r_i \cos(\theta_p - \theta_i)\right] d\theta_p \\
&= \frac{2\pi G_o}{\lambda R} \int_0^a J_0\left(\frac{2\pi r_p r_i}{\lambda R}\right) r_p dr_p = \frac{\pi a^2 G_o}{\lambda R} \frac{2J_1(\pi r)}{\pi r}
\end{aligned}$$

where  $r = r_i/\lambda F$  is the radial distance of a point in units of  $\lambda F$  in the Gaussian image plane from the Gaussian image point.

Using normalized radial distance  $r$  and normalizing the CSF to unity at the center  $r = 0$ :

$$CSF(r) = \frac{2J_1(\pi r)}{\pi r}$$

$CSF(r)$  is illustrated in Figure 2-67. Its square is the Airy pattern, representing the normalized irradiance distribution of the image of a point object.

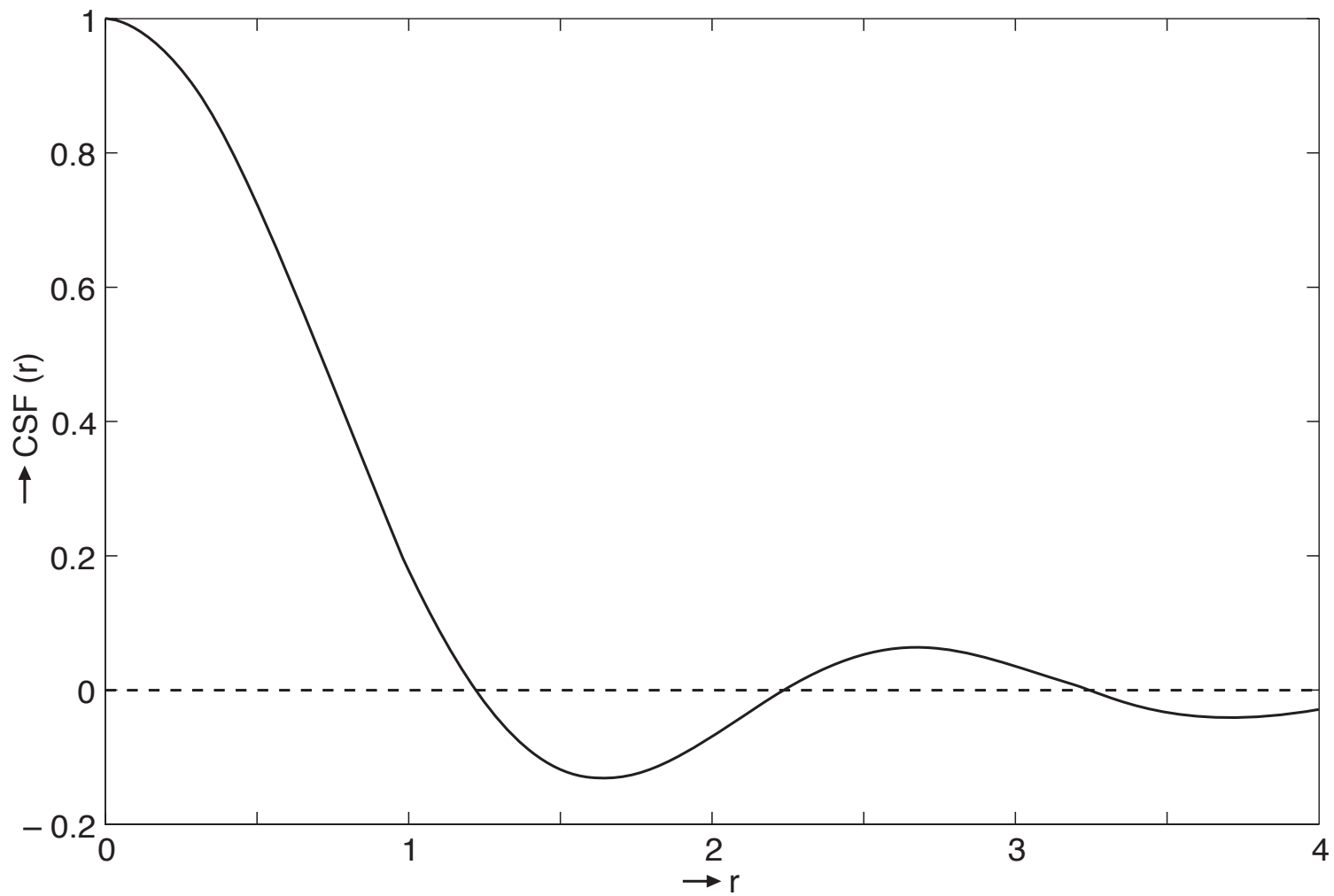


Figure 2-67. Aberration-free coherent spread function normalized to unity at the center.  $r$  is in units of  $\lambda F$ .

## Coherent transfer function

$$CTF(\vec{v}_i) = G(\lambda R \vec{v}_i)$$

For a phase aberration function  $\Phi(\vec{r}_p)$ , where  $|\vec{r}_p| \leq a$ , and uniform amplitude across the pupil:

$$CTF(\vec{v}_i) = \exp[i\Phi(\lambda R \vec{v}_i)] \quad , \quad |\lambda R \vec{v}_i| \leq a$$

For an aberration-free system, all frequencies  $|\vec{v}_i| \leq 1/2\lambda F$  are transmitted by the system without any amplitude or phase distortion.

- Spatial frequency  $|\vec{v}_{ic}| = 1/2\lambda F$  is called the **coherent cutoff frequency** of the system in the sense that object frequencies corresponding to image frequencies greater than  $1/2\lambda F$  are not transmitted by it.
- **Cutoff frequency for coherent imaging is half of that for incoherent imaging.**

Using normalized spatial frequency  $\vec{v} = \vec{v}_i/|\vec{v}_{ic}| = \vec{v}_i/(1/2\lambda F)$ :

$$CTF(\vec{v}) = \exp[i\Phi(\vec{v})] \quad , \quad |\vec{v}| \leq 1$$

## Two-Point Resolution

### Incoherently illuminated two point objects

Incoherent object:

Two point objects of equal intensity with Gaussian images separated by Rayleigh resolution  $1.22\lambda F$  and located at  $x = \pm 0.61\lambda F$ .

Aberration-free incoherent image:

$$I(x) = \left\{ \frac{2J_1[\pi(x-0.61)]}{\pi(x-0.61)} \right\}^2 + \left\{ \frac{2J_1[\pi(x+0.61)]}{\pi(x+0.61)} \right\}^2 \quad (x \text{ in units of } \lambda F)$$

- Distribution is symmetrical about  $x = 0$  with a dip at the center that has a value of 0.73 compared to a maximum value of unity at  $x = \pm 0.61$ .

Defocused incoherent image:

$$I(x; B_d) = 4 \left[ \left| \int_0^1 \exp(iB_d \rho^2) J_0[\pi(x-0.61)\rho] \rho d\rho \right|^2 + \left| \int_0^1 \exp(iB_d \rho^2) J_0[\pi(x+0.61)\rho] \rho d\rho \right|^2 \right]$$

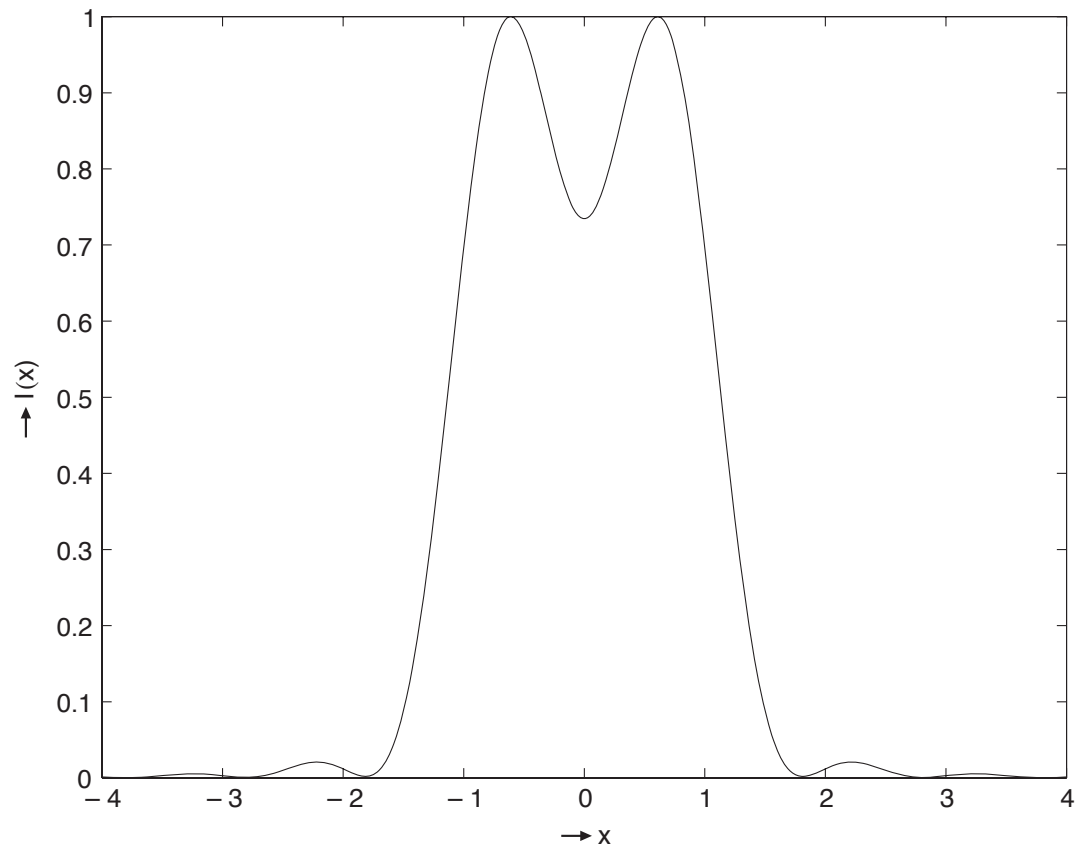


Figure 2-81. Irradiance distribution along the  $x$  axis of the image of two **incoherent** point objects of equal intensity with Gaussian images separated by the Rayleigh resolution  $1.22\lambda F$ .  $x$  is in units of  $\lambda F$ .

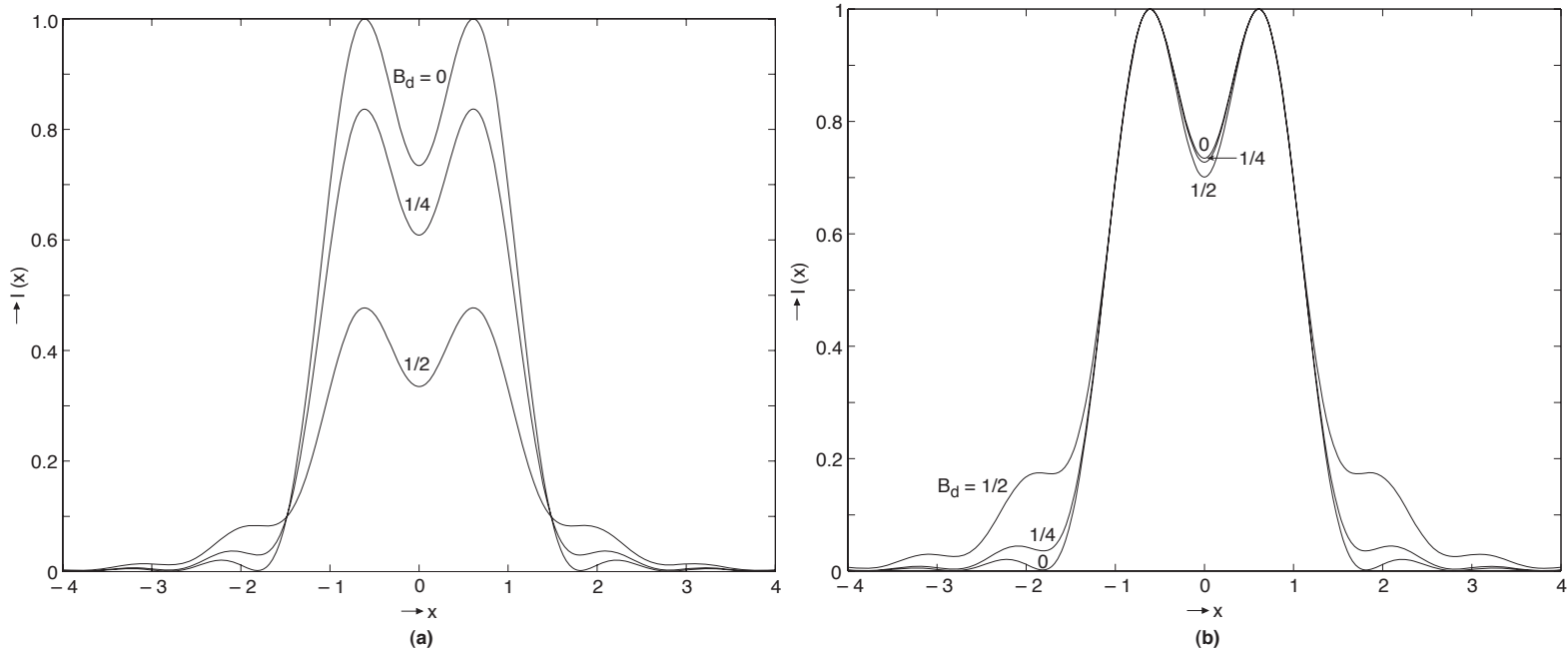


Figure 2-83. (a) Defocused image along the  $x$  axis of two **incoherent** point objects with Gaussian images separated by the Rayleigh resolution  $1.22\lambda F$ .  $B_d$  is in units of  $\lambda$  and  $x$  is in units of  $\lambda F$ . (b) Images normalized to unity at the principal peaks.

- Central values in (a) with increasing defocus are 0.73, 0.61, and 0.33, and the principal peaks have a value of 1, 0.84, and 0.48 located at  $x = \pm 0.61$ .
- Normalization of principal peaks to unity as in (b) shows that the effect of defocus on the relative dip is small.

## Coherently illuminated two point objects

Coherent object:

Two point objects of equal amplitude with a phase difference  $\delta$  and Gaussian images separated by the Rayleigh resolution  $1.22\lambda F$  and located at  $x = \pm 0.61\lambda F$ .

Aberration-free coherent image:

$$I(x) = \left| \frac{2J_1[\pi(x - 0.61)]}{\pi(x - 0.61)} + \exp(i\delta) \frac{2J_1[\pi(x + 0.61)]}{\pi(x + 0.61)} \right|^2$$

- Irradiance distribution is symmetrical about  $x = 0$ . Since  $J_1(1.22\pi) = 0$ , therefore,  $I(\pm 0.61) = 1$ , regardless of the value of  $\delta$ , as shown in Figure 2-82.
- No dip in the distribution when the point objects are in phase ( $\delta = 0$ ); hence, they can not be resolved.
- However, when their phases are opposite of each other ( $\delta = \pi$ ), then the irradiance at the center is zero, making it easier to resolve them.
- When  $\delta = \pi/2$ , then the irradiance distribution is the same as for two incoherent point objects.

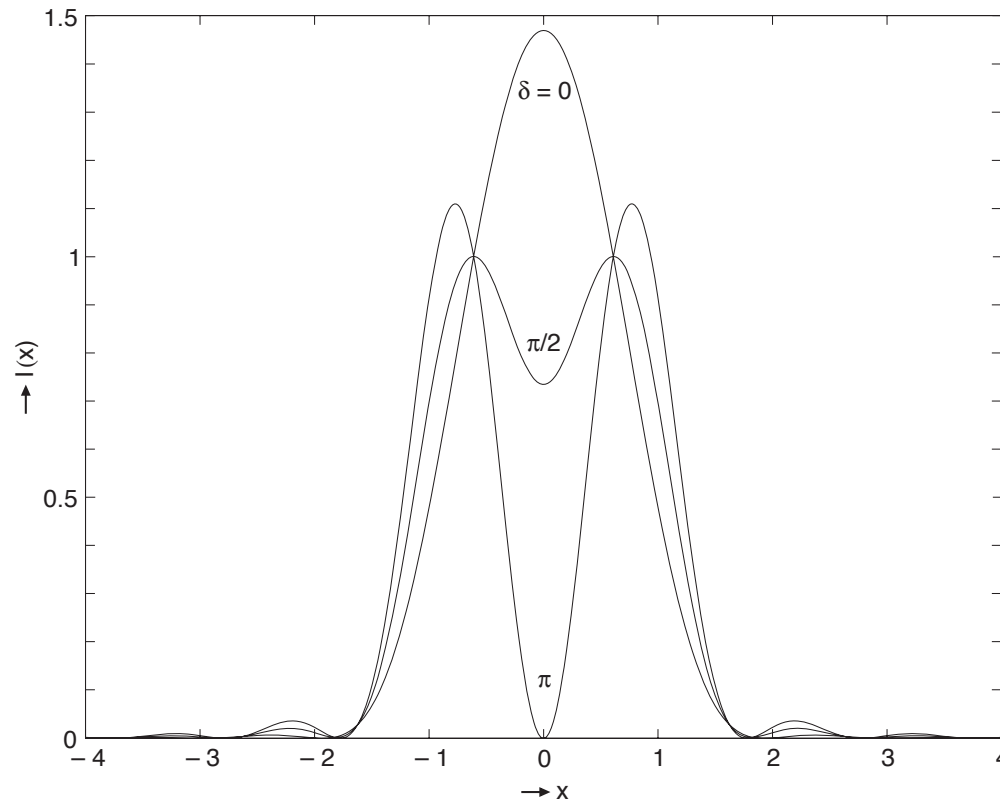


Figure 2-82. Irradiance distribution of the image of two **coherent** point objects with Gaussian images separated by the Rayleigh resolution  $1.22\lambda F$  and a relative phase  $\delta$ . The distribution for  $\delta = \pi/2$  is the same as for two incoherent point objects.

- Ability to resolve points of a coherently illuminated object is strongly dependent on the phase relation among them.

Defocused coherent image:

$$I(x) = 4 \left[ \int_0^1 \exp[i\Phi(\rho)] J_0[\pi(x - 0.61)\rho] \rho d\rho + \exp(i\delta) \int_0^1 \exp[i\Phi(\rho)] J_0[\pi(x + 0.61)\rho] \rho d\rho \right]^2$$

- Distribution is symmetric for  $\delta = 0$  and  $\pi$ .
- Central value decreases with defocus in Figure 2-84a, and the side peaks decrease in value in Figure 2-84b (the central value is zero in this case).
- However, the defocused distribution is quite asymmetric when  $\delta = \pi/2$ . Although the presence of two point objects can be inferred from this figure, one would incorrectly infer that they are of unequal intensity.
- If the defocus aberration is negative, as when  $z > R$ , then the object appearing dimmer in Figure 2-84c will lie on the right-hand side of the origin.

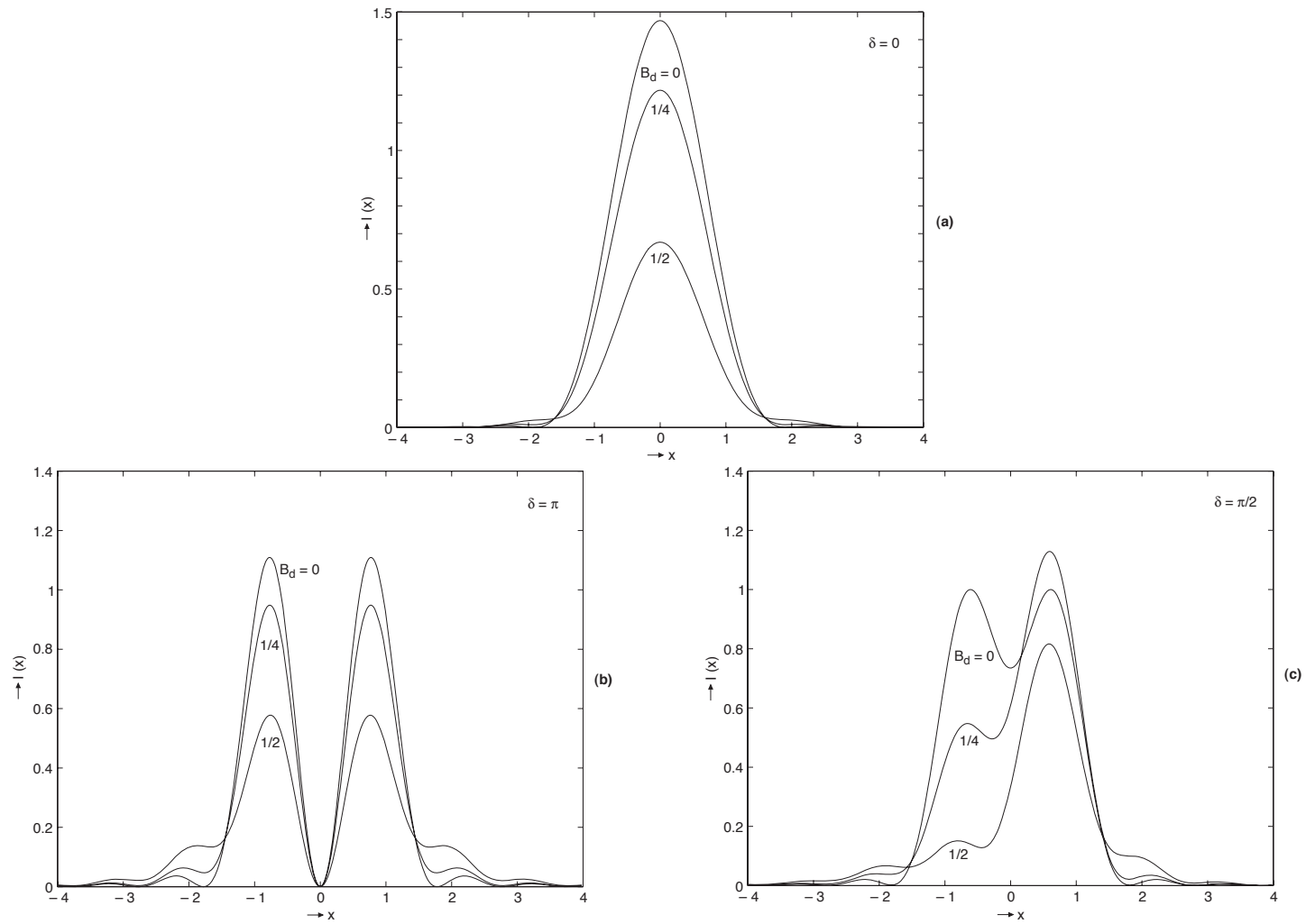
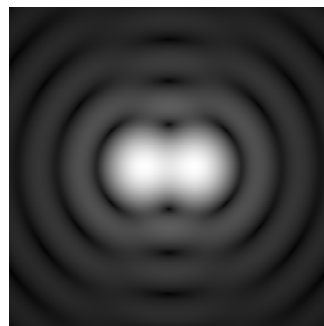
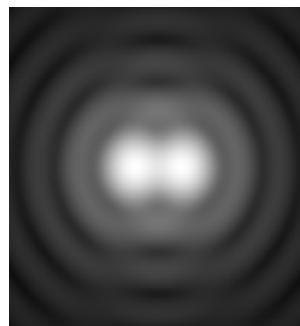


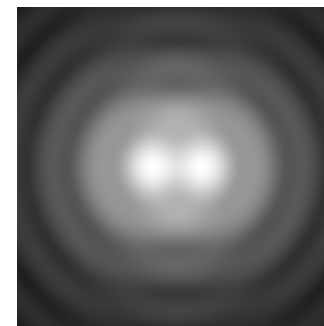
Figure 2-84. Irradiance distribution of defocused images of two **coherent** objects of equal intensity and a phase angle  $\delta$ . (a)  $\delta = 0$ . (b)  $\delta = \pi$ . (c)  $\delta = \pi/2$ .



$B_d = 0$

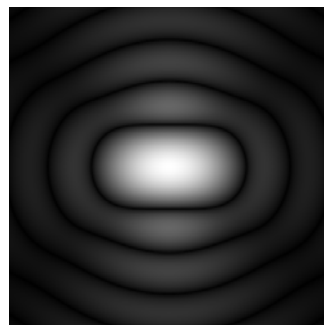


$B_d = 1/4$

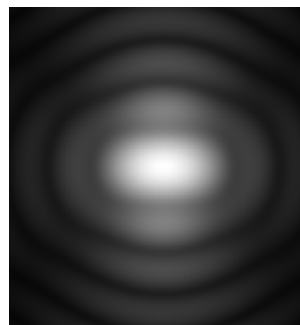


$B_d = 1/2$

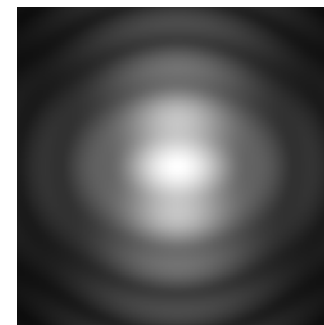
**Incoherent** points



$B_d = 0$



$B_d = 1/4$



$B_d = 1/2$

**Coherent** points in phase ( $\delta = 0$ )

Figure 2-85. Aberration-free and defocused images two object points separated by the Rayleigh resolution  $1.22\lambda F$ .

- **Coherent points can not be resolved.**

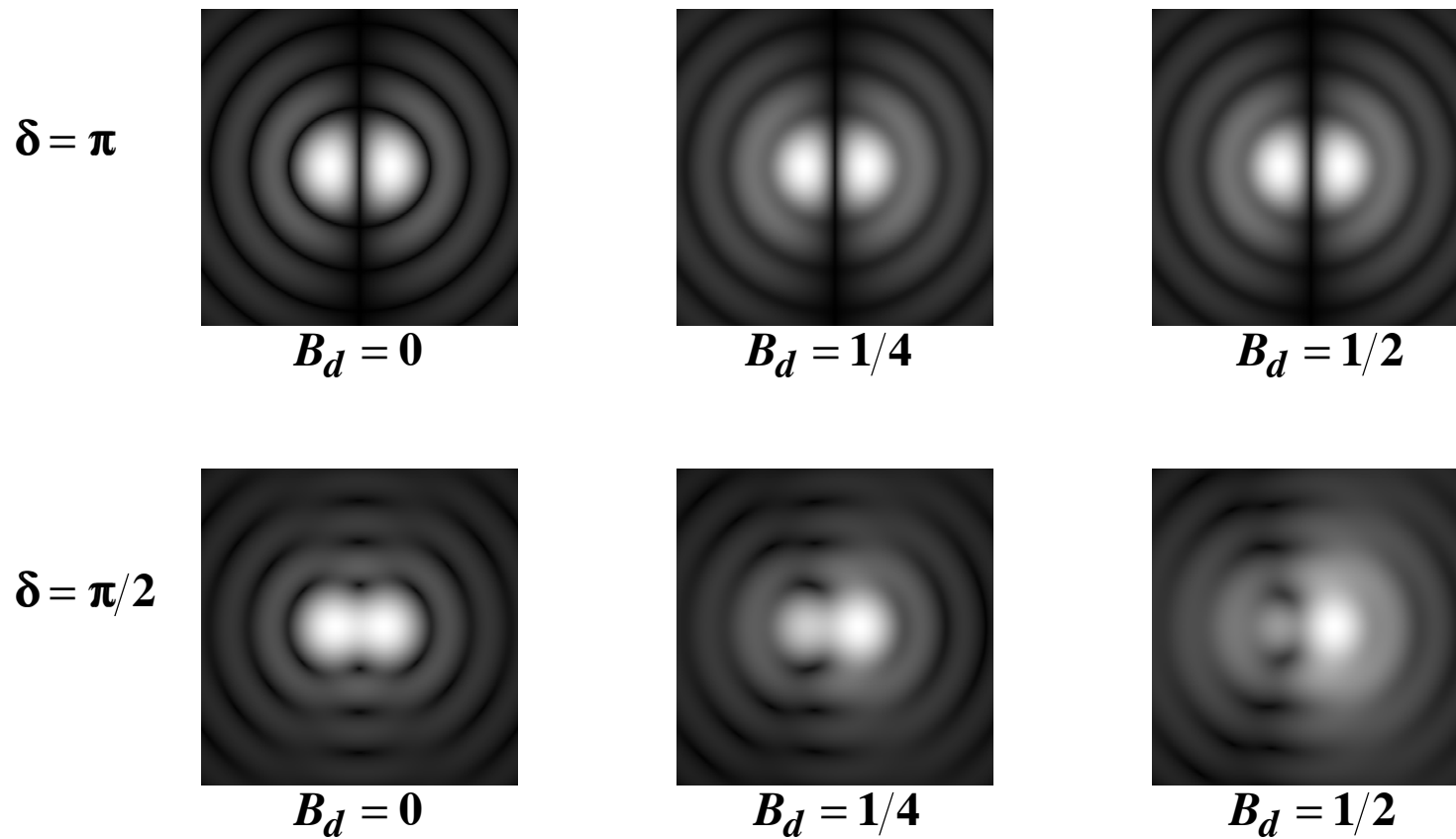


Figure 2-86. Aberration-free and defocused images of two **coherent** point objects with a phase difference  $\delta$ .

- **Defocused image incorrectly conveys point objects of unequal intensity when  $\delta = \pi/2$ .**

## Incoherent Line-Spread Function

Diffraction image of an isoplanatic extended object is given by the convolution of its Gaussian image and the system PSF:

$$I_i(\vec{r}_i) = \int I_g(\vec{r}_g) PSF(\vec{r}_i - \vec{r}_g) d\vec{r}_g$$

Object: Line object along the  $y_o$  axis.

Gaussian image:  $I_g(\vec{r}_g) = \delta(x_g)$ .

Diffraction image:

$$\begin{aligned} LSF(x_i) &= \int_{-\infty}^{\infty} \int_{-\infty}^{\infty} \delta(x_g) PSF(x_i - x_g, y_i - y_g) dx_g dy_g \\ &= \int_{-\infty}^{\infty} PSF(x_i, y_i - y_g) dy_g = \int_{-\infty}^{\infty} PSF(x_i, y_i) dy_i \end{aligned}$$

- For a line object along the  $y_o$  axis, the LSF depends only on  $x_i$ , i.e., its variation with  $x_i$  is the same regardless of the value of  $y_i$ , as expected for an isoplanatic line object.

For a radially symmetric PSF:

$$LSF(x_i) = 2 \int_0^{\infty} PSF\left(\sqrt{x_i^2 + y_i^2}\right) dy_i$$

Substituting  $r_i = \left(x_i^2 + y_i^2\right)^{1/2}$ :

$$LSF(x_i) = 2 \int_{x_i}^{\infty} \frac{PSF(r_i)}{\left(r_i^2 - x_i^2\right)^{1/2}} r_i dr_i$$

Thus, LSF is the **Abel transform** of the PSF.

Aberration-free LSF by substituting Eq. (2-15) for the Airy pattern:

$$LSF(x_i) = \frac{8}{\pi^2} \int_{x_i}^{\infty} \frac{J_1^2(\pi r_i)}{r_i \left(r_i^2 - x_i^2\right)^{1/2}} dr_i$$

- The ratio of the LSF at the origin with and without aberrations is called the **Struve ratio** and its value is  $\leq 1$ . See Table 2-16 for aberration tolerances and balancing for a certain value of Struve ratio.

## LSF from OTF

- Integration over infinite limits can be avoided by writing the LSF in terms of the system OTF:

Substituting for  $PSF(x, y)$  in terms of its Fourier transform, the OTF  $\tau(\xi, \eta)$ :

$$\begin{aligned} LSF(x) &= \int_{-\infty}^{\infty} PSF(x, y) dy \\ &= \int_{-\infty}^{\infty} dy \iint \tau(\xi, \eta) \exp[-2\pi i(\xi x + \eta y)] d\xi d\eta \\ &= \iint \tau(\xi, \eta) \exp(-2\pi i\xi x) d\xi d\eta \int_{-\infty}^{\infty} \exp(-2\pi i\eta y) dy \\ &= \iint \tau(\xi, \eta) \exp(-2\pi i\xi x) \delta(\eta) d\xi d\eta \\ &= \int \tau(\xi, 0) \exp(-2\pi i\xi x) d\xi \end{aligned}$$

- Thus,  $LSF(x)$ , representing the image of a line object lying along the  $y_0$  axis, is the 1-D inverse Fourier transform of  $\tau(\xi, 0)$  (Theorem 21a).

Since  $LSF(x_i)$  is a real function, only the real part of the integrand contributes to the integral; the imaginary part yields zero upon integration.

$$\therefore LSF(x) = \int \operatorname{Re} \tau(\xi, 0) \cos(2\pi\xi x) d\xi - \int \operatorname{Im} \tau(\xi, 0) \sin(2\pi\xi x) d\xi$$

For the aberration-free case,  $\tau(\xi, 0)$  is real and even, and since  $-1 \leq \xi \leq 1$ :

$$LSF(x) = 2 \int_0^1 \tau(\xi, 0) \cos(2\pi\xi x) d\xi$$

$$\text{where } \tau(\xi, 0) = \frac{2}{\pi} \left[ \cos^{-1} \xi - \xi (1 - \xi^2)^{1/2} \right], \quad -1 \leq \xi \leq 1$$

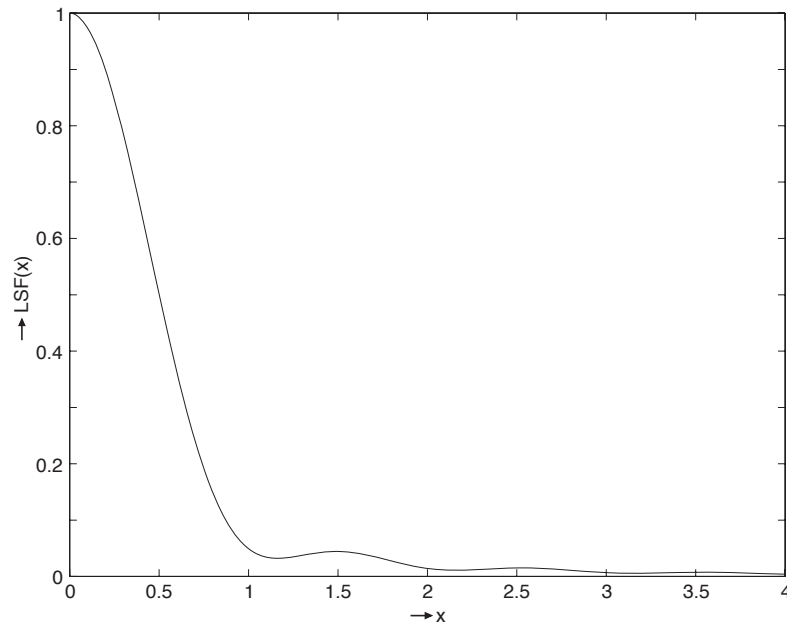
LSF at the origin:

$$LSF(0) = 2 \int_0^1 \tau(\xi, 0) d\xi = \frac{8}{3\pi}$$

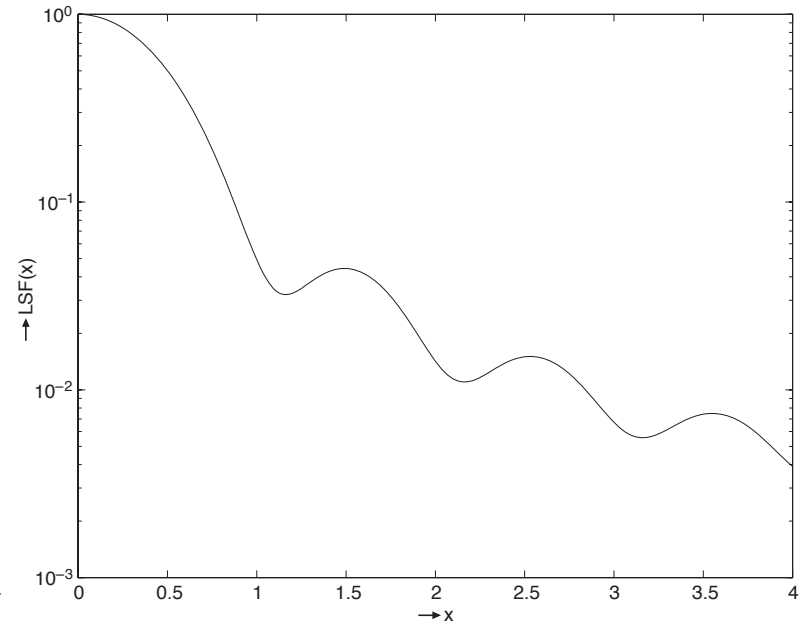
LSF normalized by its central value:

$$LSF(x) = \frac{3\pi}{4} \int_0^1 \tau(\xi, 0) \cos(2\pi\xi x) d\xi = \frac{3}{8\pi x^2} H_1(2\pi x)$$

where  $H_1(\cdot)$  is the first-order Struve function. It is symmetric about  $x = 0$ .



**(a)**



**(b)**

Figure 2-52. Aberration-free incoherent LSF normalized to unity at the center. It is symmetric about  $x = 0$ . (a) Linear scale. (b) Log scale.  $x$  is in units of  $\lambda F$ .

## Incoherent Edge-Spread Function

Image of an edge object is called the *edge-spread function* (ESF).

Edge object passing through the origin and lying parallel to the  $y_o$  axis in the left half of the space is represented by a step function:

$$\begin{aligned} H(x_o) &= 1 \quad \text{for } x_o \geq 0 \\ &= 0 \quad \text{for } x_o < 0 \end{aligned}$$

Diffraction image:

$$ESF(x_i) = \int_{-\infty}^{\infty} \int_{-\infty}^{\infty} PSF(x, y) H(x_i - x) dx dy = \int_{-\infty}^{\infty} LSF(x) H(x_i - x) dx$$

Thus,  $ESF(x_i)$  is equal to a 1-D convolution of the Gaussian image  $H(x_i)$  of the edge object with  $LSF(x_i)$ , or a 2-D convolution with  $PSF(x_i, y_i)$ , as expected for an isoplanatic extended object.

Substituting for the step function:

$$ESF(x_i) = \int_0^{\infty} LSF(x_i - x_g) dx_g = \int_{-\infty}^{x_i} LSF(x) dx = \int_{-\infty}^{x_i} dx \int_{-\infty}^{\infty} PSF(x, y) dy$$

- LSF is the derivative of the ESF (since ESF is the integral of LSF), i.e.,

$$LSF(x_i) = \frac{d}{dx_i} ESF(x_i)$$

$$ESF(\infty) = \int_{-\infty}^{\infty} dx \int_{-\infty}^{\infty} PSF(x, y) dy = 1$$

### ESF from OTF:

Fourier transform the convolution expression for the ESF.

$$\int LSF(x) \exp(2\pi i \xi x) dx = \tau(\xi, 0)$$

$$\int H(x) \exp(2\pi i \xi x) dx = \frac{\delta(\xi)}{2} - \frac{1}{2\pi i \xi}$$

$$\begin{aligned} \therefore \int ESF(x) \exp(2\pi i \xi x) dx &= \tau(\xi, 0) \left[ \frac{\delta(\xi)}{2} - \frac{1}{2\pi i \xi} \right] \\ &= \frac{\delta(\xi)}{2} - \frac{\tau(\xi, 0)}{2\pi i \xi} \quad [\text{since } \tau(0, 0) = 1] \end{aligned}$$

Inverse Fourier transforming:

$$ESF(x) = \frac{1}{2} - \frac{1}{2\pi i} \int \frac{\tau(\xi, 0)}{\xi} \exp(-2\pi i \xi x) d\xi$$

Thus,  $ESF(x)$  and  $\tau(\xi, 0)/\xi$  are related to each other by a 1-D Fourier transform (Theorem 21b).

For an incoherent object,  $ESF(x)$  is a real function. Hence, only the imaginary part of the integrand contributes to the integral; the real part yields zero upon integration.

$$\therefore ESF(x) = \frac{1}{2} + \int \operatorname{Re} \tau(\xi, 0) \frac{\sin(2\pi \xi x)}{2\pi \xi} d\xi - \int \operatorname{Im} \tau(\xi, 0) \frac{\cos(2\pi \xi x)}{2\pi \xi} d\xi$$

ESF at the origin:

$$\begin{aligned} ESF(0) &= \frac{1}{2} - \int \frac{\operatorname{Im} \tau(\xi, 0)}{2\pi \xi} d\xi \quad (\text{determined solely by the imaginary part}) \\ &= \frac{1}{2} \quad \text{when the OTF is real, as for a symmetric aberration,} \\ &\quad \text{regardless of the type and the value of the aberration.} \end{aligned}$$

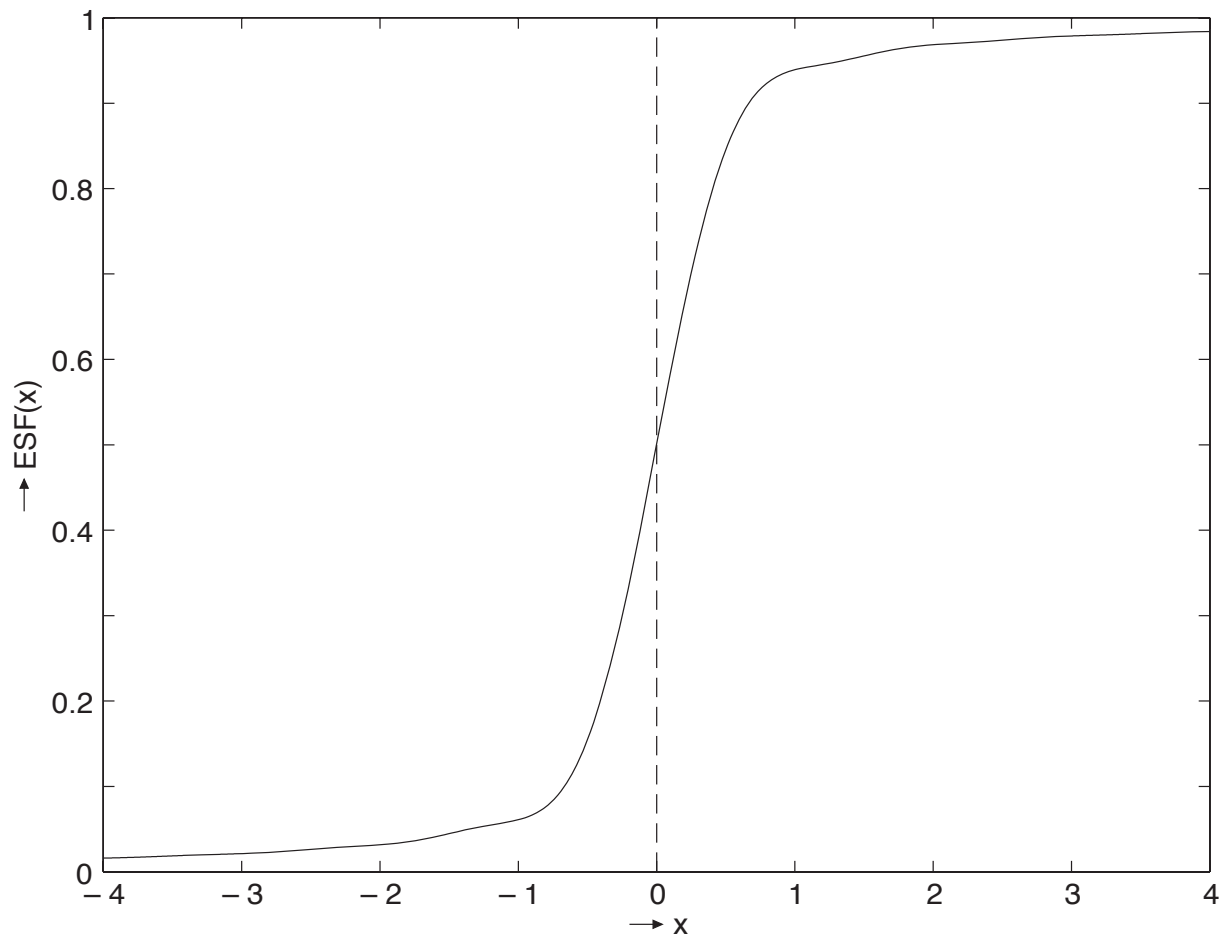


Figure 2-55. Aberration-free incoherent ESF. The Gaussian image of the edge has a value of zero for  $x < 0$  and unity for  $x \geq 0$ . It is indicated by the vertical dashed line.  $x$  is in units of  $\lambda F$ .

## Coherent LSF and ESF

Amplitude image of an isoplanatic coherent line or an edge object is given by the convolution of its Gaussian image and the coherent point-spread function CSF.

Hence, equations for the incoherent LSF and ESF of a system in terms of its OTF are also applicable to coherent imaging, provided the OTF is replaced by the corresponding coherent transfer function (CTF).

$$LSF_{\text{coh}}(x) = \int \tau_{\text{coh}}(\xi, 0) \exp(-2\pi i \xi x) d\xi$$

$$ESF_{\text{coh}}(x) = \frac{1}{2} - \frac{1}{2\pi i} \int \frac{\tau_{\text{coh}}(\xi, 0)}{\xi} \exp(-2\pi i \xi x) d\xi$$

For an aberration function  $\Phi(x, y)$ , the CTF is given by

$$\tau_{\text{coh}}(\xi, 0) \equiv CTF(\xi, 0) = \exp[i\Phi(\xi, 0)]$$

where  $\xi$  is in units of  $\xi_c = 1/2\lambda F$ .

## Coherent LSF

LSF for a line object along the  $y_o$  axis:

$$LSF(x) = \frac{1}{2} \int_{-1}^1 \exp\{i[\Phi(\xi, 0) - \pi\xi x]\} d\xi \quad (x \text{ in units of } \lambda F)$$

- Division by 2 normalizes the aberration-free LSF to unity at the origin.

LSF for an even aberration, such as defocus or astigmatism is complex, but symmetric about  $x = 0$ :

$$LSF(x) = \int_0^1 \exp[i\Phi(\xi, 0)] \cos(\pi\xi x) d\xi \quad ()$$

LSF for an odd aberration, such as coma, is real:

$$LSF(x) = \int_0^1 \cos[\Phi(\xi, 0) - \pi\xi x] d\xi$$

Aberration-free system:

$$LSF(x) = \frac{\sin \pi x}{\pi x}$$

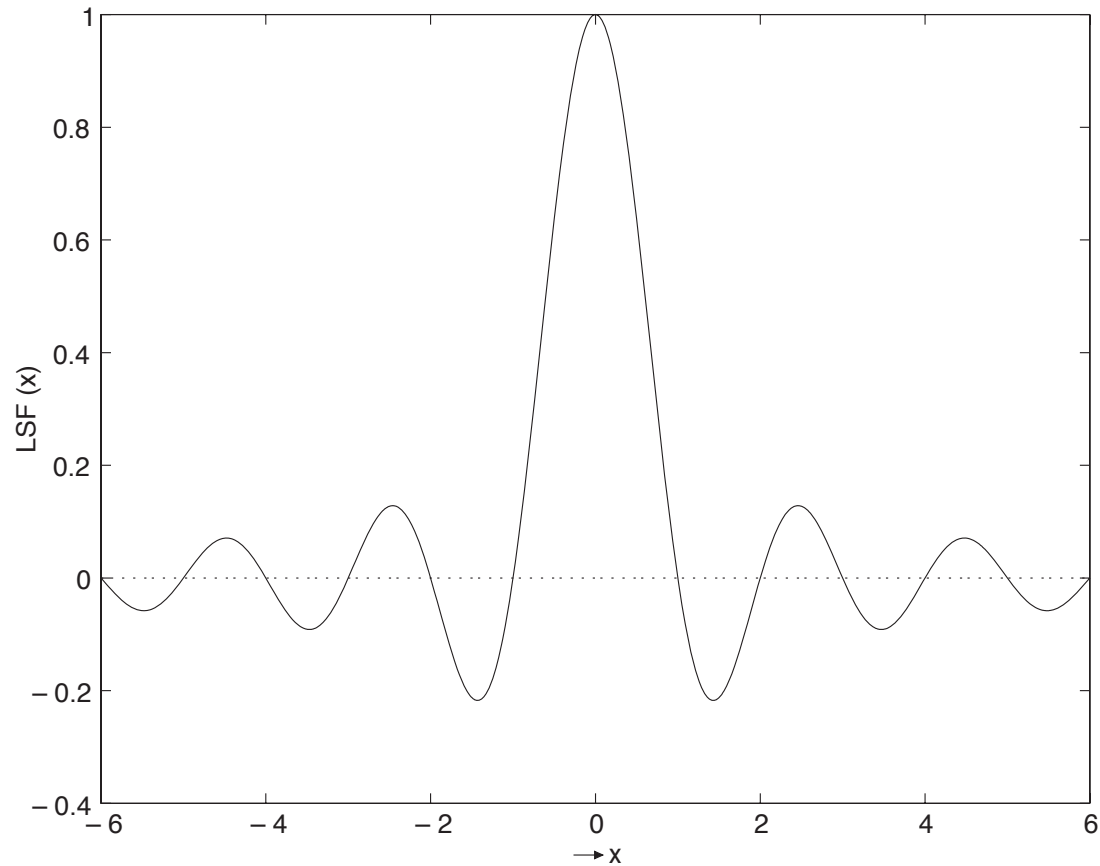


Figure 2-68. Aberration-free coherent LSF normalized to unity at the center.  $x$  is in units of  $\lambda F$ .

Coherent LSF is zero for  $x = \pm n$ , where  $n$  is a nonzero integer, unlike the incoherent LSF (compare with Figure 2-52).

## Coherent ESF

$$ESF(x) = \frac{1}{2} - \frac{1}{2\pi i} \int_{-1}^1 \exp\{i[\Phi(\xi, 0) - \pi\xi x]\} \frac{1}{\xi} d\xi$$

Aberration-free system:

$$ESF(x) = \frac{1}{2} + \int_0^1 \frac{\sin(\pi\xi x)}{\pi\xi} d\xi$$

ESF maxima and minima occur at integral values of  $x$ .

Its value at  $x = 0$  is 0.5, and its principal maximum lies at  $x = 1$  with a value of 1.09 (see Figure 2-72).

It approaches unity as  $x \rightarrow \infty$ , and 0 as  $x \rightarrow -\infty$ .

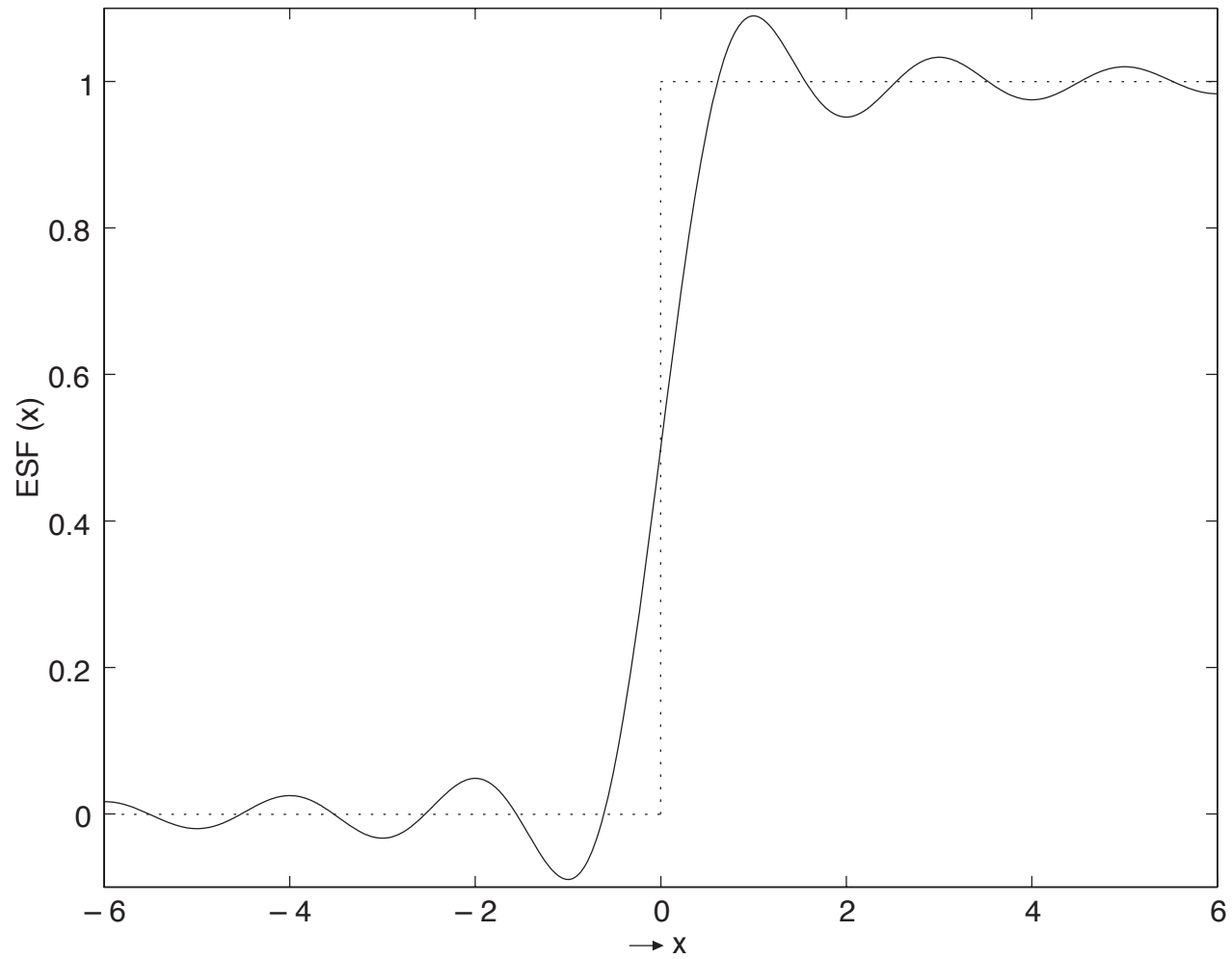


Figure 2-72. Aberration-free coherent ESF.  $x$  is in units of  $\lambda F$ . The dotted curve represents the Gaussian image of the edge object.

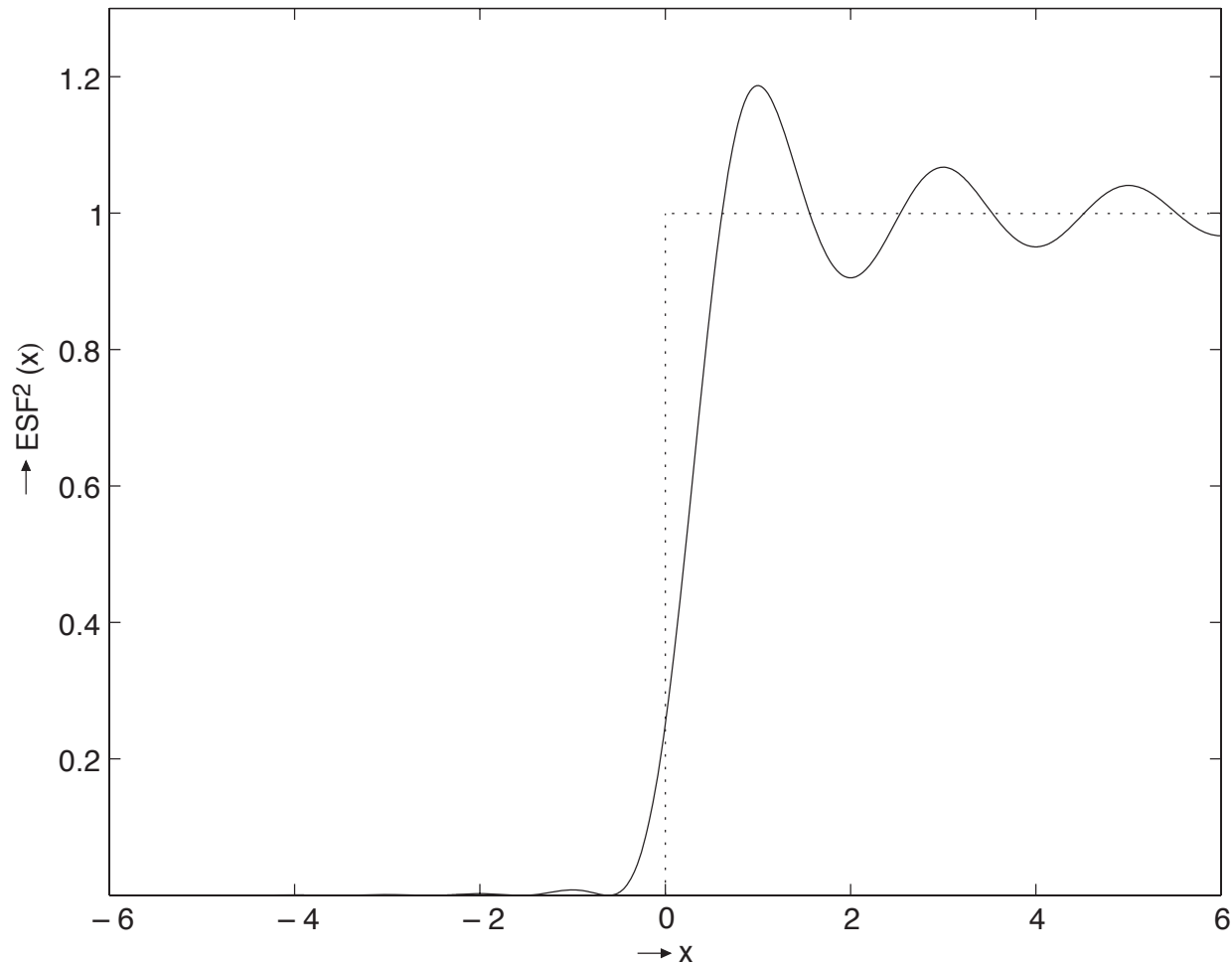


Figure 2-73. Irradiance distribution associated with the aberration-free coherent ESF.  $x$  is in units of  $\lambda F$ . The dotted curve represents the Gaussian image of the edge object.

Irradiance distribution associated with the aberration-free ESF has a value of 0.25 at  $x = 0$  and a value of 1.19 at the principal maximum at  $x = 1$ .

It is evident from Figure 2-73 that the **edge appears to be shifted toward the bright region.**

There are strong fluctuations in the irradiance distribution on the bright side of the Gaussian image of the edge. Such fluctuations are absent in the incoherent ESF shown in Figure 2-55.

Moreover, the spatial period of the fluctuations on the dark side (shadow region) is half of that on the bright side. It results from the squaring operation of the positive and negative fluctuations of the amplitude ESF on the dark side.

- **Aberrated incoherent and coherent LSF and ESF are given in the book.**

## Image of an Incoherent Disc

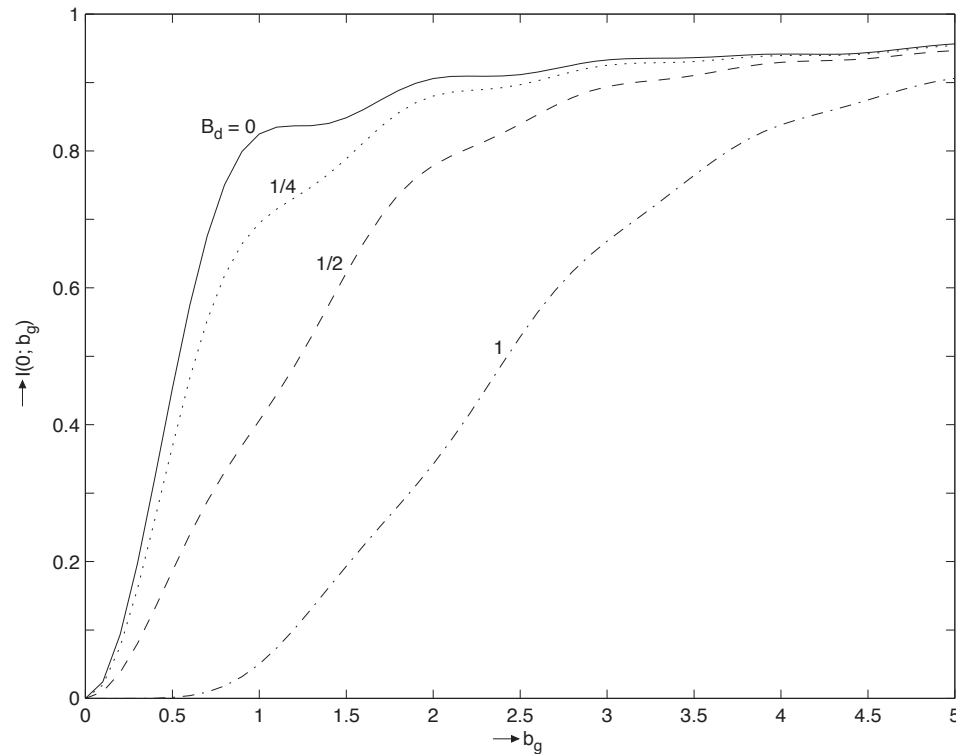


Figure 2-62a. Central irradiance of a defocused image of a uniformly illuminated incoherent disc. Its Gaussian image radius  $b_g$  is in units of  $\lambda F$  and the defocus coefficient  $B_d$  is in units of  $\lambda$ .

- Central irradiance approaches unity (actually irradiance  $I_g$  of the Gaussian image) asymptotically.

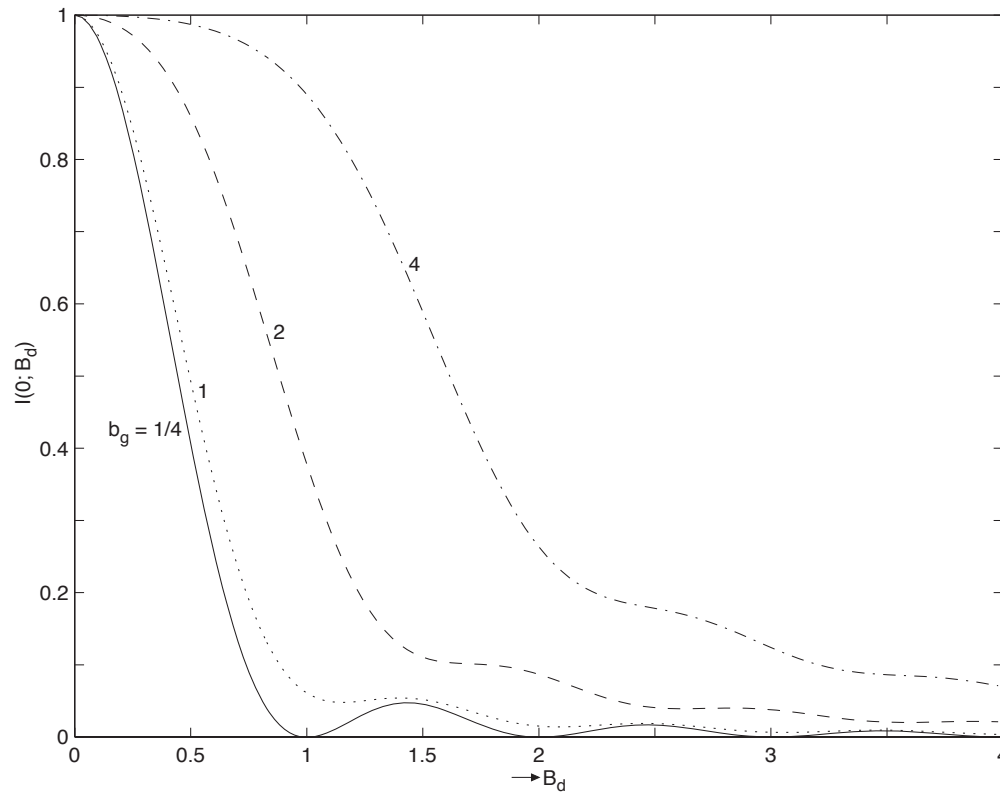


Figure 2-62b. Axial irradiance of an incoherent disc normalized to unity at the center. The actual central values (normalized by  $I_g$ ) in increasing order of  $b_g$  are 0.14, 0.825, 0.91, and 0.94.

- For  $b_g = 1/4$ , axial irradiance is approximately the same as for a point source. For example, it is nearly zero for integral values of  $B_d$  (in units of  $\lambda$ ). It becomes nonzero for larger discs.

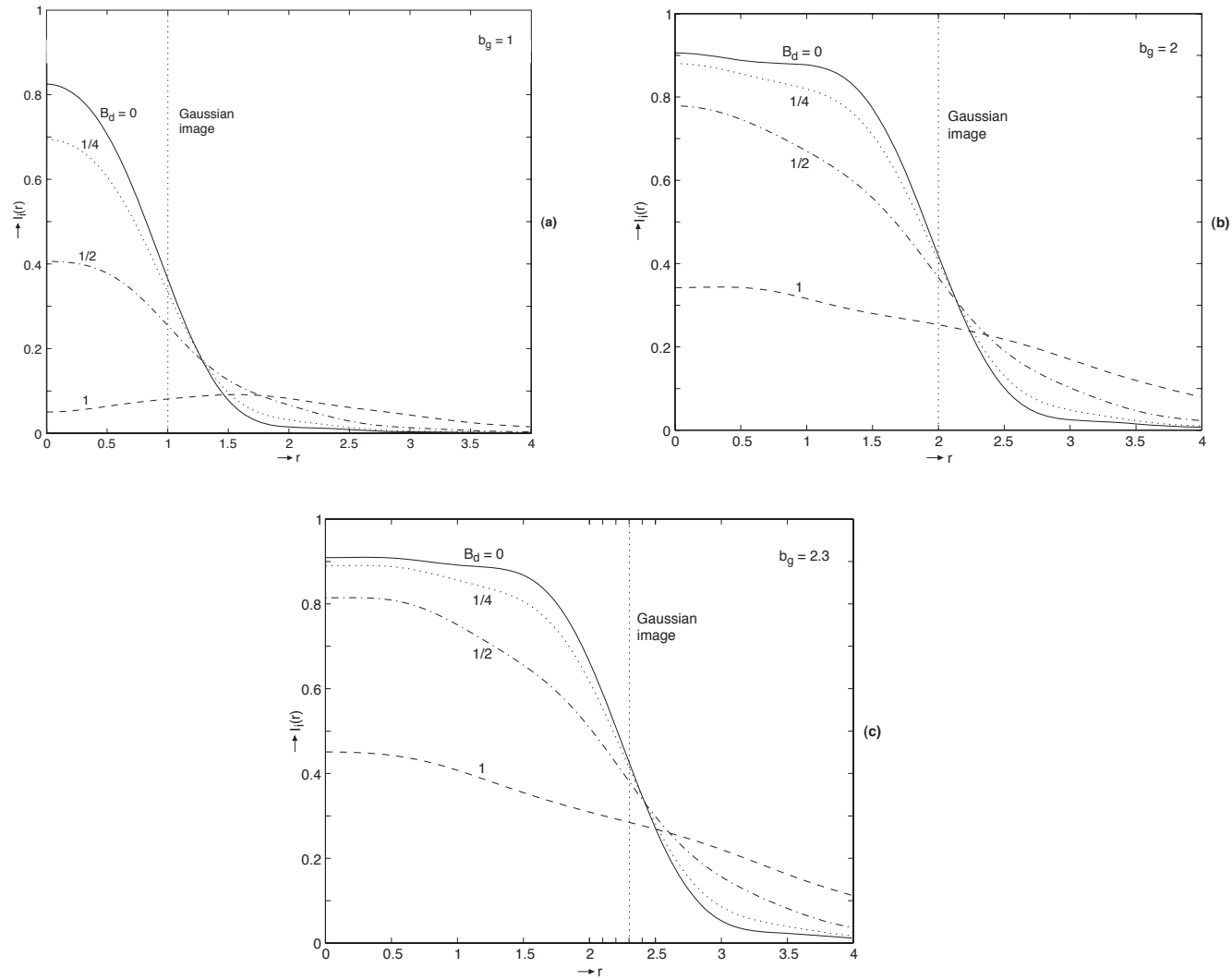


Figure 2-63. Irradiance distribution of defocused images of an incoherent disc. Gaussian image of radius  $b_g$  is indicated by the dashed vertical line.

- Image generally resembles the object. In particular, it is bright in the central region and dim in the outer region.
- As defocus increases, the irradiance decreases in the central region and increases in the outer region.
- If the disc is small and the defocus is large, the irradiance at the center may be smaller than that in the outer region as, for example, for  $b_g = 1$  and  $B_d = 1\lambda$ . This behavior is similar to that for a point source, and it disappears as the disc size increases.
- Central irradiance of the image of a **coherently** illuminated disc can be much lower than that in the surrounding region, whether or not the image is defocused (unless the disc is very small like a point object).
- Moreover, defocus can increase the central irradiance, as illustrated in Figures 2-76 and 2-77.

## Image of a Coherent Disc

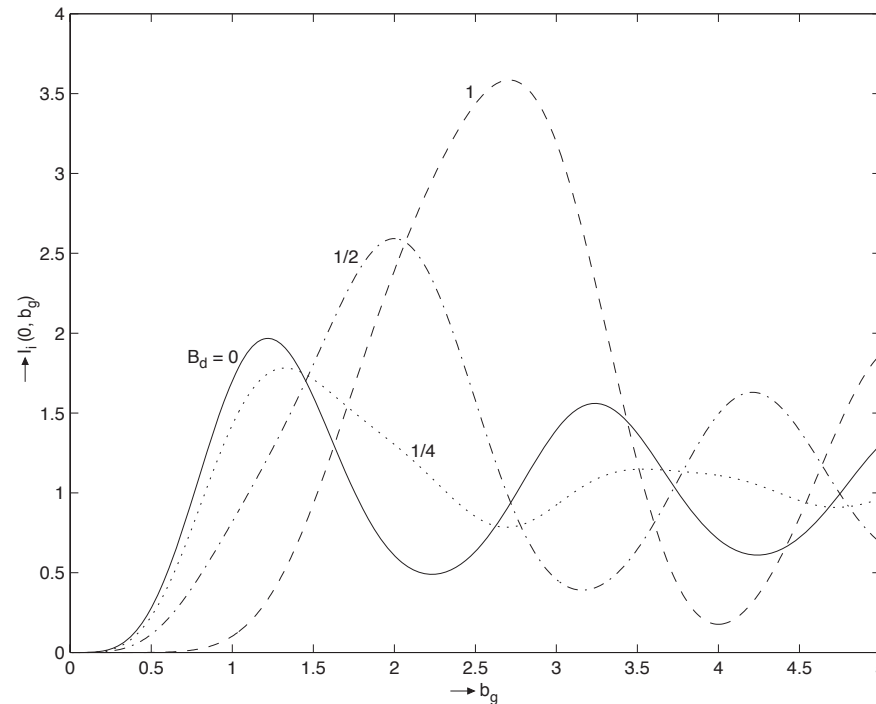


Figure 2-76a. Central irradiance of the defocused image of a coherent disc.

- For small discs  $b_g \leq 1.3$ , the aberration-free central irradiance is higher than a corresponding defocused value.
- However, for larger discs, the aberration-free value is not necessarily higher than a defocused value.

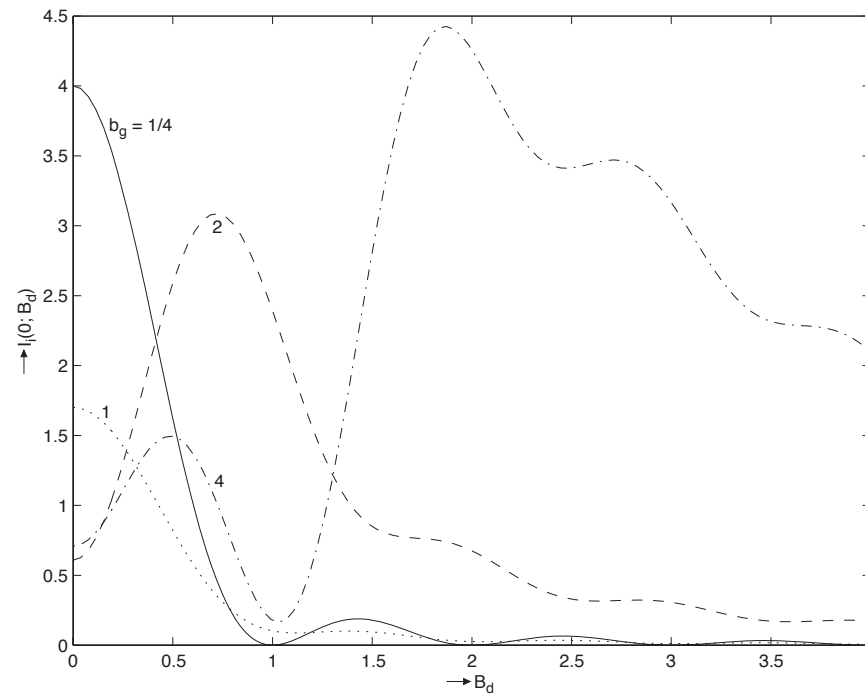


Figure 2-76b. Axial irradiance of a coherent disc. The central value in the case  $b_g = 1/4$  is normalized to 4 to accentuate the secondary maxima. The actual central values in increasing order of  $b_g$  are 0.02, 1.70, 0.61, and 0.71.

- For a small disc, the irradiance is maximum at the center of its image. It behaves like a point source for  $b_g = 1/4$ . For a large disc, the maximum occurs at a defocused point, as evidenced by the curves for  $b_g = 2$  and 4.

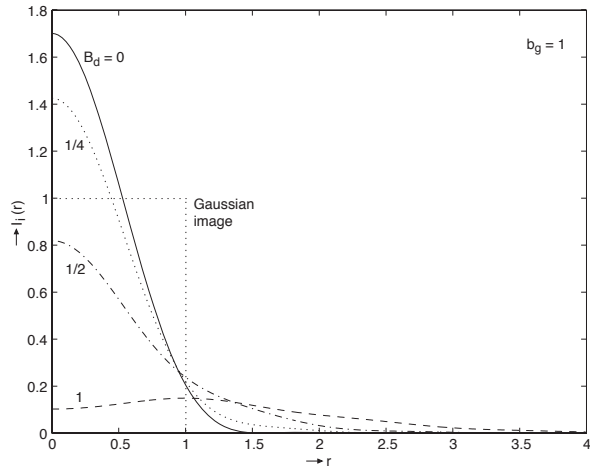
Figure 2-77a shows the defocused images for  $b_g = 1$ . The aberration-free image looks more like the Gaussian image compared to the defocused images.

Figure 2-77b shows the defocused images for  $b_g = 2$ . The aberration-free image has a dip in the middle of the image and does not resemble the Gaussian image.

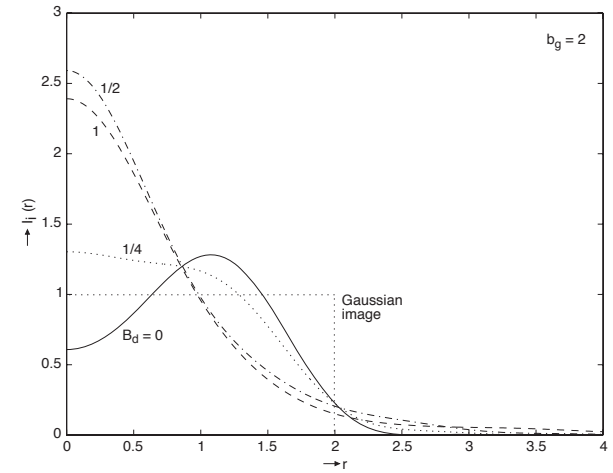
Moreover, the **central value for a defocus of one wave is much larger than the corresponding aberration-free value, contrary to the case of an incoherent disc** [Compare with Figure 2-63b].

It is a coincidence that, for the disc size under consideration, the image for a half wave of defocus is similar to that for one wave of defocus. They are quite different, for example, for  $b_g = 2.3$ , as may be seen from Figure 2-77c.

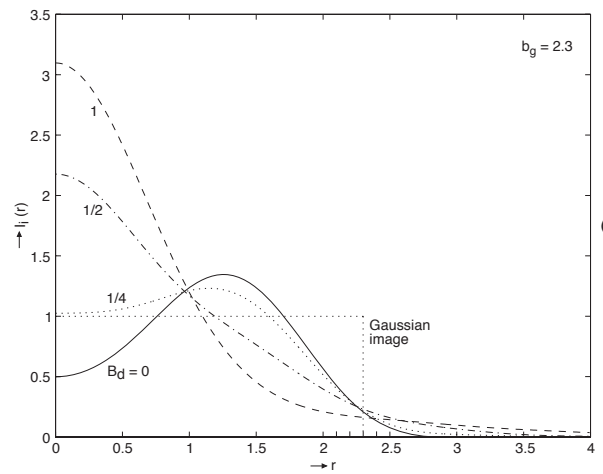
It is evident that, whereas the **image of an incoherent disc resembles the object, the image of a coherent disc can be quite different from it.**



(a)



(b)



(c)

Figure 2-77. Irradiance distribution of the defocused images of a coherent disc whose Gaussian image radius is  $b_g$  in units of  $\lambda F$ . The Gaussian image is indicated by the dotted curve.

**Unusual behavior of the coherent disc images may be explained qualitatively as follows:**

If we divide the disc into narrow radial zones (similar to the Fresnel zones), the parts of a given zone contribute to the central amplitude in phase, since they are equidistant from the image center.

However, different zones do not contribute in phase, since they lie at different distances from the image center (unless the phase difference between the contributions of two zones happens to be  $2\pi$ ).

Complex amplitudes contributed by different zones can partially cancel each other. This cancellation may be reduced by the defocus aberration, resulting in a larger defocused central irradiance.

Relative phase of a zone does not matter in the case of an incoherent disc, because the phases of contributions from different zones are randomly related to each other, and it is the irradiance contributions from different zones that are added to obtain the net irradiance.

Hence, the central irradiance increases as the radius of an incoherent disc increases.

## Image of an Extended Object

As an example of incoherent and coherent images of an extended object with a given imaging system, diffraction-limited images of Taj Mahal are shown in Figure 2-80.

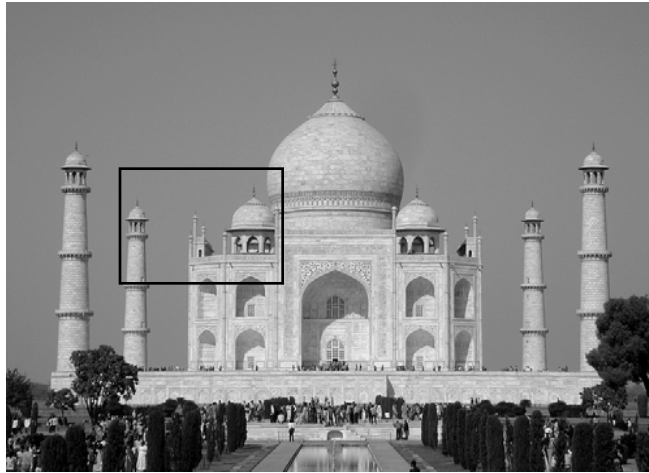
For clarity, a magnified image of its boxed portion only is shown.

Incoherent image, corresponding to a solar-illuminated Taj, is definitely better than the coherent image corresponding to a laser-illuminated Taj.

Edge ringing associated with coherent imaging is quite evident in the coherent image.

Incoherent image is relatively smooth.

If a diffuser is placed between the laser and the object, the image breaks up into small random spots called *speckles*.



Object



Incoherent Image



Coherent Image

Figure 2-80. Incoherent and coherent images of Taj Mahal built by the Mughal Emperor Shah Jahan. For clarity, a magnified image of its boxed portion only is shown. The edge ringing associated with coherent imaging is quite evident in the coherent image.

## Use of a Lens for Obtaining Fourier Transforms

If the amplitude of a wave in the plane  $z = 0$  is  $U(\vec{r}'; 0)$ , then its amplitude in the  $z$ -plane in the Fraunhofer region  $z > kr_{\max}'^2/2$  is given by its Fourier transform:

$$U(\vec{r}; z) = \frac{-i}{\lambda z} \exp\left[ik\left(z + \frac{r^2}{2z}\right)\right] \int U(\vec{r}'; 0) \exp\left(-\frac{2\pi i}{\lambda z} \vec{r} \cdot \vec{r}'\right) d\vec{r}' \quad (1-23a)$$

- Accordingly, if an object transparency of radius  $a$  is illuminated by a plane wave, a Fourier transform of its amplitude transmittance function is obtained in the Fraunhofer region  $z > D^2/\lambda$ .
- The larger the value of  $z$ , the better the approximation of obtaining a Fourier transform.
- Since  $\lambda$  is very small, the distance  $z$  beyond which a Fourier transform is obtained can be quite large. For example,  $z \gtrsim 1$  km for  $D = 2$  cm and  $\lambda = 0.5 \mu\text{m}$ .

- This distance can be reduced by the use of a lens. The Fourier transform is obtained in the focal plane of the lens, where the plane wave illuminating the object transparency is focused by it.
- It should be clear, though, that the **Fourier transformation is a characteristic of the wave propagation and not a property of the lens**. The lens merely collapses the Fraunhofer region to its focal plane.
- Of course, an image of the transparency is obtained in the image plane determined by Gaussian optics.
- However, this image can be altered by **spatial filtering** of the complex amplitude representing the spatial-frequency spectrum of the object in the focal plane.
- Lenses used to obtain and observe Fourier transforms of objects are called **Fourier lenses**. It is difficult to design lenses that are aberration free simultaneously for the Fourier and the image planes.

The image of an object by a thin lens of focal length  $f$  lying at a (numerically negative) distance  $z_o$  from it is formed at a distance  $z_g$  with a magnification  $M$  given by

$$\frac{1}{z_g} - \frac{1}{z_o} = \frac{1}{f} \quad , \quad \vec{r}_g = M\vec{r}_o \quad , \quad z_g = Mz_o$$

Complex amplitude due to an object element of area  $d\vec{r}_o$  of unit amplitude in a plane at a distance  $z_i$  from the lens:

$$dU_i(\vec{r}_i; \vec{r}_o; z_i) = -\frac{i}{\lambda z_i} \exp\left\{ ik \left[ (z_i - z_g) + \frac{1}{2} \left( \frac{r_i^2}{z_i} - \frac{r_o^2}{z_o} \right) \right] \right\} \\ \times \int G(\vec{r}_p; \vec{r}_o; z_i) \exp\left[ -\frac{2\pi i}{\lambda} \vec{r}_p \cdot \left( \frac{\vec{r}_i}{z_i} - \frac{\vec{r}_g}{z_g} \right) \right] d\vec{r}_p$$

Defocused relative pupil function:

$$G(\vec{r}_p; \vec{r}_o; z_i) = G(\vec{r}_p; \vec{r}_o) \exp\left[ \frac{ik}{2} \left( \frac{1}{z_i} - \frac{1}{z_g} \right) r_p^2 \right]$$

Complex amplitude in the focal plane is obtained by letting  $z_i = f$  and  $\vec{r}_i = \vec{r}_f$ :

$$G(\vec{r}_p; \vec{r}_o; f) = G(\vec{r}_p; \vec{r}_o) \exp \left[ ik \left( \frac{1}{f} - \frac{1}{z_o} \right) r_p^2 \right] = G(\vec{r}_p; \vec{r}_o) \exp \left( - \frac{ik}{z_o} r_p^2 \right)$$

$$dU_f(\vec{r}_f; \vec{r}_o; f) = - \frac{i}{\lambda f} \exp \left\{ ik \left[ (f - z_o) + \frac{1}{2} \left( \frac{r_f^2}{f} - \frac{r_o^2}{z_o} \right) \right] \right\} \\ \times \int G(\vec{r}_p; \vec{r}_o) \exp \left( - \frac{ik}{2z_o} r_p^2 \right) \exp \left[ - \frac{2\pi i}{\lambda} \vec{r}_p \cdot \left( \frac{\vec{r}_f}{f} - \frac{\vec{r}_o}{z_o} \right) \right] d\vec{r}_p$$

If the system is aberration free and the lens is quite large, we may replace  $G(\vec{r}_p; \vec{r}_o)$  by a constant that is directly proportional to the object element area  $d\vec{r}_o$  and inversely proportional to the distance of the object  $z_o$  from the entrance pupil, and extend the region of integration to infinity.

The integral becomes the inverse Fourier transform of an imaginary Gaussian function evaluated at the spatial frequency  $(\vec{r}_f f^{-1} - \vec{r}_o z_o^{-1})/\lambda$ :

$$\int G(\vec{r}_p; \vec{r}_o) \exp \left( - \frac{ik}{2z_o} r_p^2 \right) \exp \left[ - \frac{2\pi i}{\lambda} \vec{r}_p \cdot \left( \frac{\vec{r}_f}{f} - \frac{\vec{r}_o}{z_o} \right) \right] d\vec{r}_p \rightarrow \frac{id\vec{r}_o}{f} \exp \left[ \frac{ikz_o}{2} \left( \frac{\vec{r}_f}{f} - \frac{\vec{r}_o}{z_o} \right)^2 \right]$$

Complex amplitude in the focal plane for an object of transmittance  $U_o(\vec{r}_o)$  illuminated by a plane wave of uniform amplitude (ignoring unessential phase factors):

$$U_f(\vec{r}_f; f) = \frac{1}{f} \exp\left[\frac{ik}{2}\left(1 + \frac{z_o}{f}\right)\frac{r_f^2}{f}\right] \int U_o(\vec{r}_o) \exp\left(-\frac{ik}{f}\vec{r}_f \cdot \vec{r}_o\right) d\vec{r}_o$$

- It is **proportional to a Fourier transform of the amplitude object** and a measurement of the irradiance distribution yields the power spectrum of the object.
- Phase factor varying as  $r_f^2$  vanishes when the object is placed in the front focal plane of the lens (so that  $z_o = -f$ ). The image is formed at infinity in this case, and a second lens must be used to observe it in its focal plane.
- For a high-quality Fourier transform *and* the image of an object, the lens must be aberration free for forming the image of the source illuminating the object (e.g., aberration-free focusing of the plane wave) and for forming the image of the object; i.e., it must be aberration free for two conjugates.

## Final Test